Additive Manufacturing 22 (2018) 176–186

Contents lists available at ScienceDirect

Additive Manufacturing

journal homepage: www.elsevier.com/locate/addma

An investigation into 3D printing of fibre reinforced thermoplastic composites

L.G. Blok*, M.L. Longana, H. Yu, B.K.S. Woods

Bristol Composites Institute (ACCIS), University of Bristol, Bristol, BS8 1TR, UK

ARTICLE INFO

Keywords:
Composite
Thermoplastic
3D printing
Additive manufacture

ABSTRACT

Fused filament fabrication (FFF) is a 3D printing technique which allows layer-by-layer build-up of a part by the deposition of thermoplastic material through a nozzle. The technique allows for complex shapes to be made with a degree of design freedom unachievable with traditional manufacturing methods. However, the mechanical properties of the thermoplastic materials used are low compared to common engineering materials. In this work, composite 3D printing feedstocks for FFF are investigated, wherein carbon fibres are embedded into a thermoplastic matrix to increase strength and stiffness. First, the key processing parameters for FFF are reviewed, showing how fibres alter the printing dynamics by changing the viscosity and the thermal profile of the printed material. The state-of-the-art in composite 3D printing is presented, showing a distinction between short fibre feedstocks versus continuous fibre feedstocks. An experimental study was performed to benchmark these two methods. It is found that printing of continuous carbon fibres using the MarkOne printer gives significant increases in performance over unreinforced thermoplastics, with mechanical properties in the same order of magnitude of typical unidirectional epoxy matrix composites. The method, however, is limited in design freedom as the brittle continuous carbon fibres cannot be deposited freely through small steering radii and sharp angles. Filaments with embedded short carbon microfibres (~100 μm) show better print capabilities and are suitable for use with standard printing methods, but only offer a slight increase in mechanical properties over the pure thermoplastic properties. It is hypothesized that increasing the fibre length in short fibre filament is expected to lead to increased mechanical properties, potentially approaching those of continuous fibre composites, whilst keeping the high degree of design freedom of the FFF process.

1. Introduction

Carbon fibre reinforced plastics (CFRPs) provide excellent mechanical properties and allow for significant design tailorability. A fundamental CFRP manufacturing challenge, however, is the combination of the reinforcement fibres into the polymer matrix with good consolidation, control of fibre orientation and low cost [1]. While a wide range of manufacturing methods for composites are available, most CFRP parts are formed in a two-stage process, i.e. material lay-up followed by consolidation. For the second stage, pressure needs to be applied over the entire part surface area which requires expensive equipment and increases manufacturing costs. In this work, fused filament fabrication (FFF) is investigated as an alternative CFRP manufacturing approach for low to medium production volumes and highly customizable parts, e.g. rapid prototyping, personalised devices or structures with complex geometry.

Additive manufacturing techniques, such as FFF, commonly known as 3D printing, have an underappreciated similarity to those of traditional composite materials, as both are inherently based on stacking a series of discrete layers. It is therefore reasonable to suggest that successful adaptation of 3D printing technologies to composite materials could enable a simple composite manufacturing method with lower production cost and a high degree of automation. As reinforcements can be accurately placed, the laminated structure of composite parts can be further optimised in each layer, allowing for an increase in design freedom and mechanical performance. While still a relatively undeveloped avenue of research, there is at least one company developing commercial 3D printers capable of processing continuous fibre reinforced composite materials: MarkForged [2]. The Mark One and Mark Two printers developed by MarkForged print continuous carbon fibre reinforced Nylon with mechanical properties an order of magnitude higher than common 3D printers, and open new applications in both the personal fabrication market and in the manufacture of lightweight parts for industry.

Significant challenges remain for 3D printing of CFRPs. In addition to some process specific limitations with the MarkForged printers,

* Corresponding author.
E-mail address: lourens.blok@bristol.ac.uk (L.G. Blok).

https://doi.org/10.1016/j.addma.2018.04.039
Received 30 November 2017; Received in revised form 8 March 2018; Accepted 30 April 2018
Available online 08 May 2018

which will be discussed in further detail below, there are more fundamental issues which need addressing. For example, there are currently only a few different materials available for fibre reinforced 3D printing, which limits application areas and design flexibility. The addition of (short) fibres to the printing filament increases the stiffness of the part but the strength increase is still limited as fibre pull out may occur before fibre breakage. Furthermore, current printing techniques and material options lead to the creation of significant voids in the finished parts, which have a negative impact on the obtainable strength of composites [3].

In this paper, a review is presented on the body of knowledge of 3D printing of fibre composites using the FFF technique, followed by a detailed consideration of the processing parameters which dictate the final part quality. The aim is to identify to what extent FFF may be used as a composite manufacturing method, considering along the way what progress has been made and what challenges remain. Two different methods of composite 3D printing were assessed (continuous fibre printing and short fibre printing) and comparisons were made between the two methods in terms of mechanical properties, part quality and printing versatility.

2. Review

2.1. Material extrusion processes

Material extrusion based 3D printing techniques, such as FFF and Fused Deposition Modelling (FDM), are manufacturing processes where a solid thermoplastic material is extruded through a hot nozzle. The viscous material solidifies on the build plate which allows build-up of a part with dimensional accuracies typically in the order of 100 µm [4]. The most commonly used thermoplastics for this process are acrylonitrile butadiene styrene (ABS) and polylactic acid (PLA), with typical bulk strengths between 30–100 MPa and elastic moduli in the range of 1.3–3.6 GPa [5]. Mechanical properties of 3D printed parts, however, can deviate significantly from the material bulk properties due to the specifics of how a structure is formed on the meso-scale during printing [6].

To maximise the mechanical performance of printed parts, the key elements of the printing process and how they affect final print quality must be understood (Fig. 1). Turner et al. [4,7] provide an extensive review on FFF process modelling, including the flow and thermal dynamics of the melt, the extrusion process and the bonding process between successive layers of material. Temperature, viscosity and surface energy of the melt play an important role in how the material flows through the nozzle and more importantly, how the final interface between the beads is formed.

One of the major process variables is the raster angle, as illustrated in Fig. 2, which leads to different properties across the principal

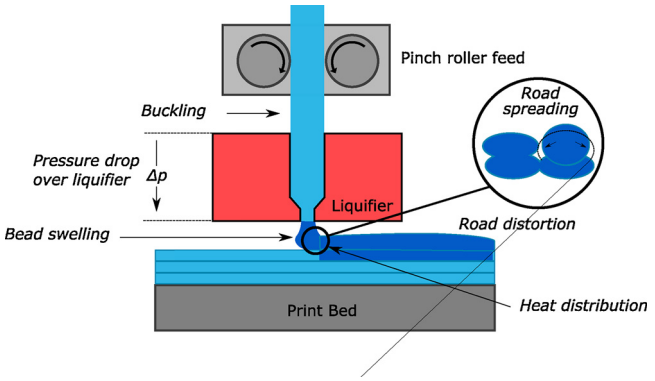

Fig. 1. Key elements of the FDM process. Adapted from [7].

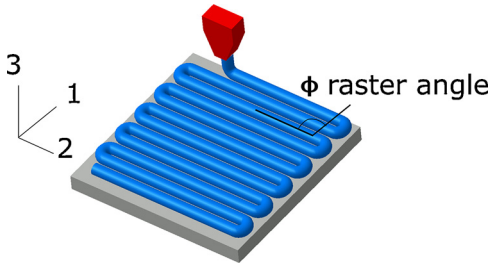

Fig. 2. Example of meso-structure of 3D printed parts with raster angle.

material directions [8–10], similar to the orthotropic behaviour of fibre composites. This allows for design tailoring, but stiffness can be 11% lower and tensile strength up to 50% lower in the weaker 1- and 3-directions compared to the bulk properties, as the interface between printed tracks can be weak [11,12].

Important features on the mesoscale are the contact area between the printed tracks and the minimization of the overall void content, as they can have a large effect on the printed part strength. Different printing patterns can be used to increase area of contact between the printed tracks and minimize the void content as shown in Fig. 3. Several studies analysed the void density in 3D printed parts, both analytically and experimentally, with changing the gap size between tracks [6,13]. A small overlap between the tracks gave the best results, with a void density of ~5% in the 1–3 plane and 27% in the 2–3 plane. Micrographs taken of 3D printed structures typically show a clear meso-structure with diamond or triangular shaped interbead voids, as shown in Fig. 3.

On a molecular level, good chemical bonding between the polymer chains inside of adjacent beads is required for effective load transfer to obtain a high strength part [3,14]. The amount of initial surface contact and the distribution of heat between two adjacent beads leads to the formation of a neck (Fig. 4) as absorptive equilibrium is reached (a lower state of overall energy by minimizing surface area). This process is inhibited by the viscosity of the material. During neck formation, diffusion of the polymer chains occurs while the viscosity of the material increases as it cools down, slowing down the neck formation and diffusion process [7]. This process is therefore sensitive to the viscosity (temperature dependent), thermal conductivity and heat capacity of the material, as well as the cooling rate (determined by external environment). A higher temperature leads to better flow of the polymer melt, improving the polymer sintering process. Similarly, a higher thermal conductivity would improve heat distribution, aiding the chemical bonding between filaments as previously deposited material heats up to improve the sintering process. At too high temperatures, however, the polymer may degrade, and dimensional accuracy may decrease because of the increased flow.

Multiple attempts have been made to numerically model the polymer sintering process based on heat transfer calculations. Early work by Yardimci et al. [14,15] presented different modelling approaches to capture the heat transfer between printed beads, but did not look at the polymer flow dynamics. Bellehumeur et al. [16] used a model based on a polymer sintering model described by Pokluda et al. [17]. This approach performed an energy balance between surface tension and viscous dissipation [17], but with the extension of temperature dependent surface tension and viscosity. Although they did not model molecular diffusion, they found that the extruded material cools too quickly for complete bonding. They also report that the convective heat transfer coefficient has a large effect on the bond formation and neck growth, where less heat transfer leads to better neck formation. However, they modelled isothermal polymer sintering and did not consider the heat transfer from the hot extruded material to the surrounding material. Bellini [18] performed extensive modelling of the entire FDM process with ceramic filled filament using four different

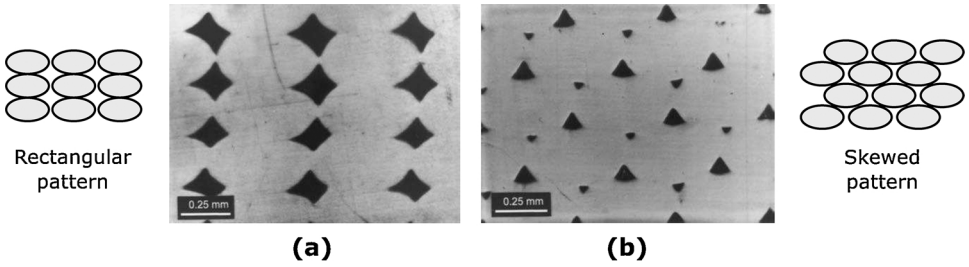

Fig. 3. Micrographs and schematics of two different meso-structures, a) rectangular and b) skewed, showing typical triangular void formation [6].

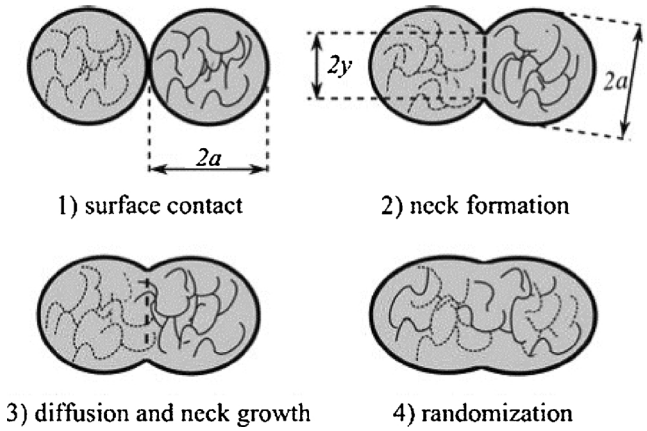

Fig. 4. Schematic overview of the polymer sintering process [7].

numerical simulations focusing on; the liquefier, the nozzle contraction, deposition on the printing bed and on stacked layers. This enabled tracking of the material temperature, swelling and filling as a function of various printing parameters. It was found that the higher thermal conductivity of the filled material increased heat transfer from the liquefier to the printed material and improved the flow behaviour.

To conclude, Fig. 5 summarises the discussed printing and material parameters that influence the print quality, mapped to the different stages of the printing process. Overall, the key to high quality parts is to obtain good surface contact and temperature conditions for optimal polymer sintering. The viscosity and surface tension of the material are important parameters, as they dictate the flow characteristics which are mainly dependent on temperature. Therefore, the heat conductivity and capacity are important, as they affect how heat is distributed and the temperature profiles of the printed tracks. Qualitatively, the main sintering process is understood and several studies focused on the effect of some of these parameters [19–21]. Of further interest is how the addition of fibre reinforcement to the feedstock will affect these parameters, this is discussed below.

2.2. Reinforced filaments for material extrusion

The FFF process can be utilized to print CFRPs by adding fibres into the thermoplastic filament. Besides the obvious motivation of increasing mechanical properties, the reinforcement may also be used to add extra functionality to the material such as electroconductivity, higher heat conductivity or biocompatibility. Kalsoom et al. [22] and Wang et al. [23] recently provided a general overview of 3D printable composite materials; this paper instead provides a more detailed focus on the engineering aspects of FFF as a composite manufacturing method. The use of fibre reinforcements in 3D printing filaments for FFF is a topic of on-going research with both advancements in scientific literature as well as in commercial products, e.g. the MarkForged printers and the numerous reinforced thermoplastic filaments available on the market [2,24,31].

Table 1 shows an overview of the different studies performed to date on printing of reinforced filaments, showing the different methodologies and resulting relevant mechanical properties. Most studies report on the use of very short carbon fibres (~0.1 mm) which are mixed with a thermoplastic polymer and then typically screw extruded to create the filament used for traditional printing. This increases the strength and stiffness of the printed material by around 65%, but this level of performance remains low compared to CFRP materials made with traditional composite manufacturing methods (e.g. pre-preg/autoclave, resin infusion, etc). High shear mixing leads to fibre breakage, reducing their length in the filament and consequently lowering the strength of the printed part [32,33].

The porosity of 3D printed short fibre composite parts has also been investigated. Three types of voids are identified by Ning et al. [24] as shown in Fig. 6. They found that the overall porosity initially decreased with the addition of fibres, but at fibre contents above 10 wt% the porosity increased to almost 10% but without distinguishing between

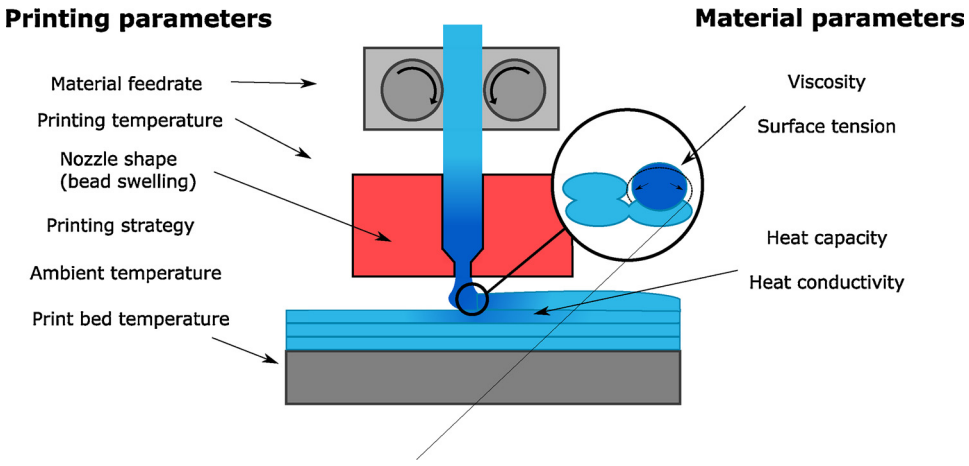

Fig. 5. Main parameters for good surface contact and temperature conditions to enable optimal polymer sintering conditions.

Table 1
Overview of studies on printing of reinforced filaments.

Study	Matrix	Reinforcement	Amount of reinforcement	Manufacturing technique	Result	Other
Ning et al. [35]	ABS	Carbon fibre powder (L = 100 μm, 150 μm and Φ = 7.2 μm)	3-15 wt%	Mixing in blender, followed by double extrusion	Strength from 34 MPa to 42 MPa, stiffness from 2 GPa to 2.5 GPa, decrease in toughness, yield strength and ductility	An increase in void content increase from 3% to 9% was recorded for 10 wt% specimens
Tekinalp et al. [25]	ABS	Short carbon fibres (L = 3.2 mm, after 0.26 mm mixing)	10,20,30,40 wt%	Mixing with torque rheometer, followed by plunger extrusion	Strength from 35 MPa to 65 MPa. Stiffness from 2 GPa to 14 GPa	For 40 wt% some nozzle clogging. Good fibre orientation for printed parts. Void content 16-27%.
Matsuzaki et al. [26]	PLA	Continuous carbon fibres and jute fibres	V_f of 6.5%	Pre-heating fibres and adding it to thermoplastic filament	Strength from 40 MPa to 185 MPa, modulus from 4 GPa to 20 GPa, with a decrease in maximum strain.	Fibres poorly distributed at the outside of the filament due to manufacturing technique, voids reported but not quantified
Shofner et al. [27]	ABS	Vapor grown carbon nanofibers L = 100 μm and Φ = 0.1 μm)	10 wt%	Sizing added to nanofibers, banbury mixing, compression moulding, granulation, screw extrusion	Strength from 26.9 MPa to 37.4 MPa and stiffness from 0.49 GPa to 0.79 GPa.	Poor adhesion between fibres and resin found by SEM pictures. Good alignment.
Mahajan and Cormier [28]	Epoxy resin	Short carbon fibres (L = 100 μm, Φ = 7.2 μm)	15 wt%	Mixing of epoxy resin and fibres, and printing via syringes	Strength from 46 MPa to 65 MPa and modulus from 2.8 GPa to 4.05 GPa.	FFT analysis was used to obtain the fibre orientation. It was found through design of experiments that fibre content, translation speed and nozzle diameter had a significant effect, while fibre length and printing pressure were less important.
Peng et al. [29]	Epoxy resin	Short glass fibres (L = 0.8 mm, Φ = 10 μm)	8 wt%	Mixing of epoxy resin and fibres and printing via syringes	Flexural modulus increase from 4.2 to 6.3 GPa and flexural modulus from 91 MPa to 109 MPa from unaligned to aligned fibres.	Similar to Mahajan and Cormier [28], writing speed was found to have a significant impact on fibre orientation.
Yang et al. [36]	ABS	Continuous carbon fibre	10 wt%	In-situ impregnation of continuous fibre through melt pool of matrix before printing	Flexural strength of 7127 MPa and flexural modulus of 7.72 GPa	Very low interlaminar shear strength of 2.81 MPa.
Lewicki et al. [31]	Epoxy resin, modified for fast curing	Carbon fibres (L = 300 and 600 μm and Φ = 6 μm)	V_f of 8%	Direct Ink Writing, mixing of resin with reinforcements using centrifugal mixer and printing using 3ml syringe	Strength of 172 MPa and stiffness from 2 GPa to 5.5 GPa.	15 wt% silica nanoparticles were added to the resin such that it behaves as a thixotropic, non-Newtonian fluid which improved flow of the fibres.

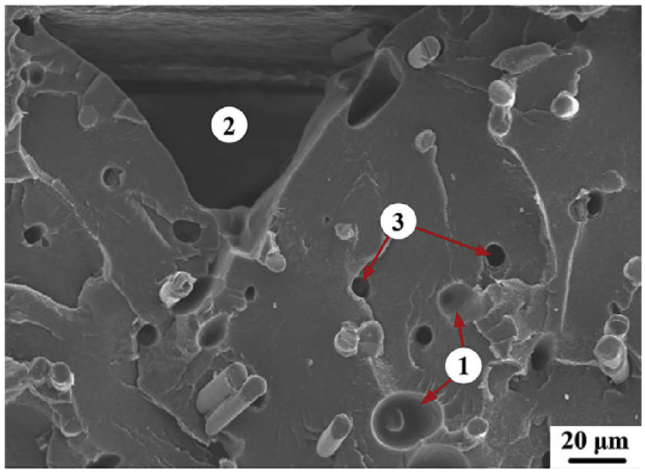

Fig. 6. Different categories of porosity in 3D printed carbon fibre composites, (1) gas bubbles (2) interbead voids and (3) fibre pull-out [35].

inter-bead voids and fibre-pull out. Tekinalp et al. [25] found a reduction of inter-bead voids with the addition of fibres, which was attributed to a decrease in die swell and increase in thermal conductivity, which helps the surrounding beads to soften and improve polymer sintering. Smaller voids, however, were found around the fibres which increased with higher fibre contents. This was attributed to a weak fibre-matrix interface and partially independent movement of the fibres and matrix during extrusion. Lastly, Zhang et al. [34] found an increase in porosity with the addition of fibres to ABS filament which shows the effect of reinforcement on the porosity is not fully understood.

Bellini [19] found numerically that a high thermal conductivity of the filled material (roughly a factor of 7 higher than unfilled material) improves heat transfer from the liquefier to the printed material, improving overall flow. The addition of fillers to the printing filament reduces die swell, as reported in three different studies [19,26,28]. The addition of fibres may be used to alter the thermal energy transfer between printed beads during deposition and the flow and the swelling behaviour of the material when leaving the nozzle.

Another promising, albeit less common, approach to 3D printing composites is to use continuous fibre reinforced filament. MarkForged has developed a printer which deposits continuous fibres (carbon, glass or Kevlar) in a Nylon matrix. The manufacture reports strength and stiffness of printed parts with carbon fibres of 700 MPa and 50 GPa respectively [2]. A ~0.4 mm diameter continuous fibre/Nylon filament is fed through a nozzle and, after it is initially anchored to the printing bed, dragged along a custom path. As it is printed, the fibre reinforced filament is transformed from an initially round cross-section to a rectangular one, with a significant amount of compression and flattening occurring to improve in-fill and inter-laminar bonding. This process, and its limitations are discussed further in the experimental section in more detail.

Yang et al. [36] developed a novel composite extrusion head, where dry carbon fibre is fed through a melt pool of ABS. This increased in-plane mechanical properties by a factor of 2–5, but a limiting factor was the interlaminar shear properties of the printed part. Matsuzaki et al. [26] printed continuous fibres (straight carbon fibres or twisted jute fibre yarns) by feeding them through a nozzle simultaneously with a thermoplastic filament (PLA) which acts as a matrix. They reported a strength and stiffness of 195 MPa and 10.5 GPa respectively which may be attributed to a low V_f of 6.6%. This technique also showed a non-uniform fibre distribution as the fibres were not pre-impregnated in the matrix.

From the review of the composite 3D printing technology presented above, two main printing methods approaches can be identified: the printing of short (0.1 mm) fibres with traditional material extrusion based printing methods and continuous fibre printing with a custom printing head and technique. Despite multiple studies available on both methods, there does not seem to be a clear consensus how these two methods compare in terms of printing versatility, print quality and mechanical properties. To better understand the two methods and how they compare, both will now be evaluated in terms of mechanical properties and printing characteristics before drawing final conclusions on how FFF may be used to manufacture cost-effective, high quality parts with good mechanical performance.

3. Experimental methodology

The part quality and mechanical performance of 3D printed composite parts manufactured using two different printing methods are investigated here. Continuous carbon fibre/Nylon 3D printed parts are made using the Mark Forged MarkOne printer and discontinuous carbon 'microfibre' reinforced Nylon parts are made using a standard desktop 3D printer. Various experiments are performed to quantify key mechanical properties, including the most detailed set of mechanical tests on the MarkOne printed parts reported to date, and optical microscopy is used to examine the quality of the parts.

3.1. MarkOne continuous fibre printer characterization

The MarkOne printer is a proprietary 3D printer which can deposit a filament made of continuous fibres embedded in a Nylon matrix. The printer has two printing nozzles as shown in Fig. 7, one to deposit pure Nylon filament, and one for fibre reinforced Nylon filament. The unreinforced Nylon nozzle is crucial for the overall integrity and quality of the prints, as the fibre filament cannot be used for the outer layers of the parts (top, bottom, sides), and for more complex shapes and thin

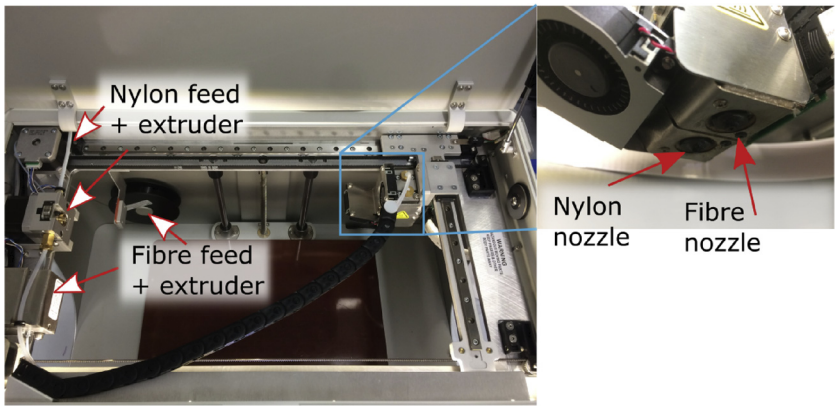

Fig. 7. Overview of the MarkOne Printer with the dual nozzle system to print Nylon filament and fibre filament.

features there often are large regions in which the fibre filament is not able to fill, which instead are filled with the unreinforced Nylon. The Nylon filament and Nylon/fibre filament are fed through Teflon Bowden tubes which run between the drive motors and the nozzles, as highlighted in Fig. 7.

To print an object, a proprietary slicing software must be used. This software is “closed source” and does not allow for user adjustment of key printing parameters such as temperature, nozzle movement or extrusion speed. This limits the printing capabilities as the printing settings cannot be fully customized. For the deposition of carbon fibres, only a circumferential fill pattern is possible which fills the shape from the outside inward in a spiralling motion. This means the fibre is always orientated along the outer perimeter of the part.

A 3D object is sliced into layers with a layer height of 0.125 mm for carbon fibre reinforced layers. The bottom and top layers are always printed with the 100% triangular fill Nylon filament, as well as the outer periphery for each layer. This is presumably done to avoid exposed fibres on the outer surface and to take advantage of the higher quality surface finish and accuracy available from the unreinforced Nylon. While this feature exists for sensible reasons, it has the negative effect of lowering the overall fibre volume fraction for the part - and thus the maximum achievable mechanical properties. Printing is done at 260 °C with at an estimated speed of 6.90 cm^3/hr for the Nylon layers and 2.39 cm^3/hr for the carbon fibre layers.

A significant downside of Nylon is that it is sensitive to water absorption, which plasticizes the matrix and can lead to a decrease in strength of up to 33% [37].

To provide a reliable and useful benchmark of the MarkOne printer, the most extensive suite of mechanical tests and printing trials reported to date were performed. The tensile, flexural and shear response of the printed material have been measured. To get around the limitations in fibre orientation caused by the circumferential fill pattern, the tensile specimens were printed in an “oval racetrack” shape to allow for two unidirectional 0° specimens to be extracted from each print, as shown in Fig. 8. The dimensions of the tensile specimens were 250 mm × 15 mm × 1 mm, sized in accordance to ASTM standard D3039 [38], where the bottom and top layers of 0.125 mm thick were 100% triangular fill Nylon as discussed above. The volume fraction of these specimens was $V_f \approx 27\%$, estimated using optical microscopy. Glass fibre tabs with a length of 25 mm were bonded to the specimen using an epoxy adhesive and the tensile test was carried out at constant displacement rate of 2 mm/min in a servo-hydraulic machine. Strain measurements were obtained from a video extensometer (IMETRUM, UK) over a gauge length of 100 mm, and the load was obtained from a 25 kN load cell (Instron).

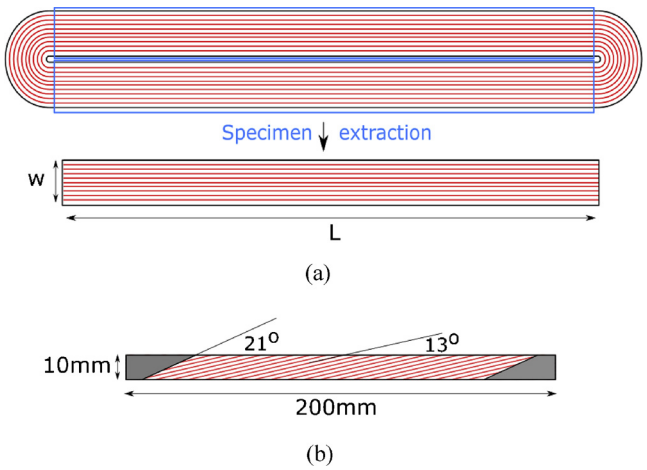

Fig. 8. Print schematic of (a) unidirectional tensile and flexural specimens and specimen extraction and (b) shear specimens, showing carbon fibre path.

A three-point bend fixture was used to obtain the flexural properties of the printed composite material with a support rod radius of 4 mm and a support length of 128 mm according to the ASTM D7264 standard [39]. The flexural specimens were manufactured in a similar approach as the tensile specimens, with outer dimensions of 160 mm × 11 mm × 4 mm and all fibres orientated in the 0° orientation. A constant displacement rate of 1 mm/min was used and the force and displacement were directly measured from the machine with a 1 kN load cell.

To obtain the shear properties, the methodology proposed by Sun and Chung [40] was used for uniaxial off-axis testing with oblique end-tabs, as a ± 45° specimen could not be printed. The oblique end tabs help create a uniform state of stress from which the shear properties can be obtained. The required oblique angle is a function of the chosen off-axis angle of the fibres and the properties of the composite, which were estimated from the results of the previous tests to be $E_{11} = 50$ GPa, $E_{22} = 0.38$ GPa, $G_{12} = 3.9$ GPa and $\nu_{12} = 0.3$. A 1 mm thick plate was printed to extract the shear samples. The sample dimensions were 200 × 10 × 1 mm, with the fibres orientated at 13°. The required angle for the oblique end-tabs for a uniform state of stress was 21° [40], as shown in Fig. 8b. The specimen was tested using an electrical-mechanical tensile machine with a 10 kN load cell and strain measurements were obtained from a 5 M P LaVision DIC system.

Lastly, to assess the printing performance of the MarkOne printer and the quality of the continuous fibres deposited, benchmark parts were printed in the form of a 40 × 40 mm square, a 30°–60°–90° triangle (85 × 50 mm) and a circle with a radius of 40 mm. Defects in printed parts due to the different geometry conditions were investigated using inspection and optical microscopy on the printed samples.

3.2. Short carbon fibre nylon filament characterization

Short fibre reinforced Nylon parts were printed using a Lulzbot TAZ 6 printer and a Nylon filament which was reinforced with chopped carbon fibres. The material was acquired from Fiberforce Italy (under the brand name Nylforce) and has 6 wt% carbon fibres added to the 3.00 mm diameter filament [41]. In comparison to the Mark One, an open-source printer allows far more control of the material deposition strategy, such as printing tracks, extrusion rate and printing temperature. To characterize this printing technique and the material, tensile, flexural and shear specimens were printed to determine the mechanical properties. Similarly, optical microscopy was used to investigate the quality of these specimens.

Tensile specimens were printed in dog-bone shapes according to the ASTM D638 [42], using a 0.4 mm nozzle diameter, 0.2 mm layer height and a printing temperature of 260 °C as recommended by the filament manufacturer. A 0° fill pattern was used such that the gauge section of the dog-bone specimens consists of tracks aligned in the 0° direction as shown in Fig. 9. The flexural specimens were printed as rectangles with dimensions 168 × 13 × 4 mm to match the ASTM D7264 standard for three point bending [39] with a support length of 128 mm. Shear samples were printed based on the ASTM D3518 standard for in-plane shear of composites, with the geometry of a dogbone and a $[\pm 45]_{8s}$ layup. The x- and y- strain components were measured at the gauge section using a video extensometer to obtain the shear modulus and strength. To assess the printing performance with the carbon fibre/Nylon filament, similar benchmark parts to the MarkOne benchmark parts were printed to investigate the corner radii and quality.

4. Results

4.1. MarkOne continuous fibre printer characterization

The results of the tensile tests on the specimens printed by the MarkOne printer are shown in Fig. 10a. Four composite samples were tested which show an average strength and stiffness of 986 MPa

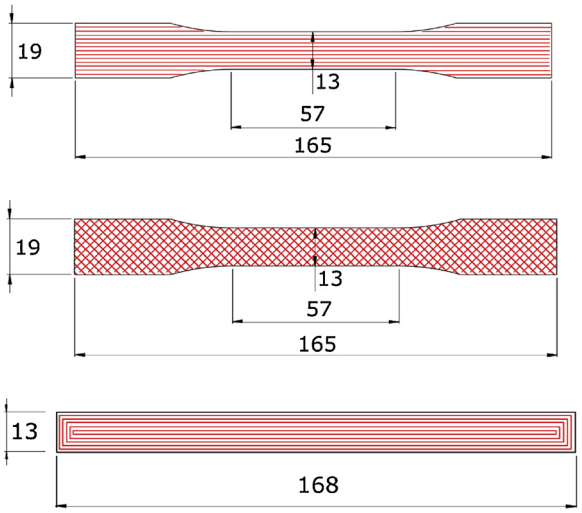

Fig. 9. Dog-bone, shear and flexural specimen printing fill patterns and specimen dimensions.

(± 8.3%) and 62.5 GPa (± 4.9%) respectively, which are higher than reported by MarkForged [2]. During the test, characteristic high frequency fibre fracture sounds were heard at a low stress of 200 MPa, after which no fracture was heard before failure. In Fig. 13a, a slight stiffening effect can be seen where the slope increases at higher strains. This may indicate early fibre fracture of possibly wrinkled fibres, followed by relaxation of most the fibres which leads to better alignment at higher load levels.

The results of the flexural tests are shown in Fig. 10b. The flexural modulus and strength of the carbon specimens are 41.6 GPa (± 4.3%) and 485 MPa (± 1.0%) respectively. The flexural strength is lower than the tensile strength which indicates there may be issues with the quality of the specimen, as a higher flexural strength is expected for high quality fibre composites [43]. A compressive failure was found for these specimens relating to a poor fibre/matrix interface and/or a high void content as failure initiators.

The shear response of the off-axis unidirectional specimens is shown in Fig. 10c. The modulus has been determined from the initial linear part of the curve, which was found to be 2.26 GPa (± 4.9%) and is lower than the predicted value of 3.9 GPa. The predicted value was used to determine the oblique end-test tab angle to obtain a uniform stress state. The difference may influence the results as a non-uniform state of stress occurs which can lead to premature failure. The maximum shear stress was 31.16 MPa (± 15.8%) where it must be noted that specimen 2 failed near the tab, which may explain its lower shear stress.

The printing quality of the MarkOne can be seen in Fig. 11 with the printing of various generic shapes. The MarkOne printer prints the carbon fibres as a continuous path which spirals from the outside contour to the inside. For more complex geometries, this causes large fibreless areas as shown in the triangular part. These fibreless areas can be up to 2.5 mm × 1 mm, which are recognized by the printing software and are partially filled with pure Nylon, but this leads to a local weakness in the part. For a simpler shape, such as a square, a similar effect is present in the corner regions on a smaller scale (1.5 mm × 0.3 mm) but the areas are not filled with Nylon here which leads to voids. For the circular shape, the fibres neatly follow the outside contour with some small gaps with a width of 0.05 mm.

Optical microscopy was performed to further asses the printing quality of the MarkOne printer. Fig. 12 shows the unprinted fibre reinforced filament, which has a nominal diameter of 400 µm. The carbon fibres seem to be localised in three bands and some voids can be seen as dark spots. The V_f in the filament was estimated using ImageJ software with a greyscale threshold and was found to be 20%.

Fig. 13 is a micrograph of the cross section of one of the flexural test specimens showing the multiple stacked layers through the thickness of the part. Within each layer distinct regions of Nylon, fibre, and void can be seen. The fibre volume content is estimated to be 27% over the cross section, which is higher then in the filament which is attributed to possible non-uniformity of the filament. Additional voids may be created during the printing process as the filament is non-uniform, forming airgaps between tracks. A void content of 7–11% was estimated from the micrograph using ImageJ and a greyscale threshold. Moreover, a non-even distribution of fibres can also be seen in the printed tracks.

4.2. Carbon fibre nylon filament characterization

The result of the tensile tests and flexural tests on the short carbon fibre Nylon filaments are shown in Fig. 14. The average tensile strength and stiffness are 33.5 MPa (± 2.7%) and 1.85 GPa (± 6.1%) respectively. The properties are lower than the bulk properties of Nylon [44], showing that the fibres do not reach their ultimate strengths. The flexural strength and stiffness were found to be 55.3 MPa (± 3.4%) and 3.0 GPa (± 4.1%) respectively. For the reinforced carbon fibre Nylon filament, the flexural strength is higher than the tensile strength, which is expected for a high quality composite part [43]. The shear results are shown in Fig. 14c. The shear strength and modulus were found to be 19.02 MPa and 0.31 GPa, respectively. One comment here is that this test method assumed orthotropic ± 45° layers, while clearly the short carbon fibre Nylon part behaved more like a plastic part, with a large amount of plastic deformation.

Fig. 15 shows the micrographs of parts printed with short carbon fibre reinforced Nylon. The printed part (Fig. 15a) shows characteristic triangular voids between the printed tracks from the FFF process. Using ImageJ software and a greyscale threshold, the total void content was estimated at 1.1%, with mainly triangular voids from the printing process).

Fig. 15b shows a 90° corner region of a printed part, showing the change in orientation of the fibres. It also shows that considerable fibre pull-out has occurred during cutting and polishing of the sample – indicating a low fibre-matrix adhesion. Some voids are present, but the gap between the printed tracks is much smaller compared to the continuous fibre filament (Fig. 11).

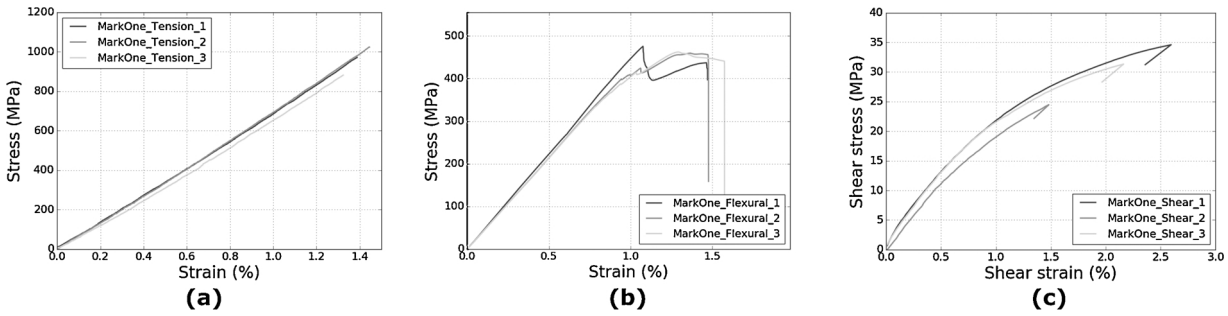

Fig. 10. Tensile, flexural and shear test results of MarkOne continuous fibre printed specimens.

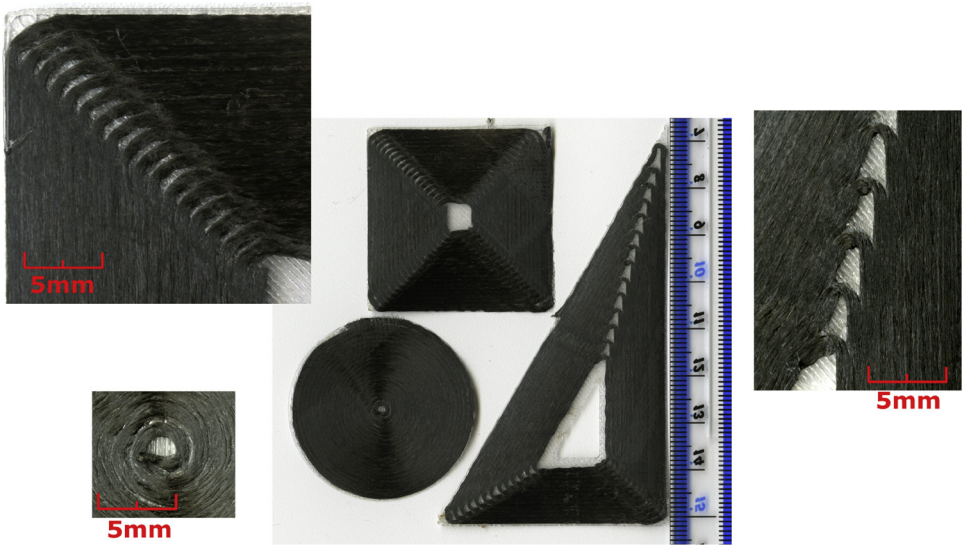

Fig. 11. Benchmark prints for MarkOne printer with detail of corner radii.

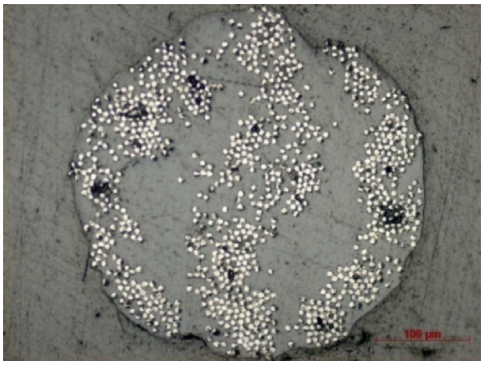

Fig. 12. Cross section of the MarkForged carbon fibre filament.

4.3. Comparison of continuous fibre printing and short fibre printing

Table 2 shows a comparison of the printing methods, where the mechanical properties have been normalised by ratio to a Vf of 15%. The tensile properties of the continuous fibre 3D printed samples were roughly an order of magnitude larger, which can be attributed to the fact that the short fibres did not reach their full strength. The flexural properties of the continuous fibre parts were lower than the tensile properties, indicating quality issues [43]. The flexural properties of the short fibre 3D printed parts were higher than its tensile properties, but still a factor 3 lower compared to the continuous fibre printing method. The shear properties of both printing methods are closer together, with the short fibre parts showing a relatively high shear strength. Together with the lower porosity, it shows that the short fibre printing method produces a higher quality part than the continuous fibre printing method.

5. Discussion

Fused filament fabrication has been investigated as a low-cost manufacturing method for fibre reinforced composites materials. An important aspect of composite materials is the consolidation of the fibres into the matrix. Traditional automated composite manufacturing techniques such as automated tape placement (ATP) use additional consolidation rollers and an autoclave process to improve the final part quality [45]. Compared to ATP machines, 3D printers are simple in design and use but lack the ability to apply additional pressure and heat to the part.

From the current body of work on composite 3D printing it must be concluded that the quality of a 3D printed part is still low compared to classical aerospace grade composite materials, as literature and this study showed void contents in the order of 10% are not uncommon for 3D printed parts. Multiple studies report on an increase in mechanical properties from unreinforced to reinforced filament, but to be used as a structural material the absolute strength and stiffness must increase as well as the consistency and quality of manufactured parts.

The coupled thermo-fluid-mechanics of the material extrusion 3D printing process has been carefully analysed to identify a method forward to improve the quality of 3D printed composite parts. The basic extrusion process is well documented, but the literature lacks a

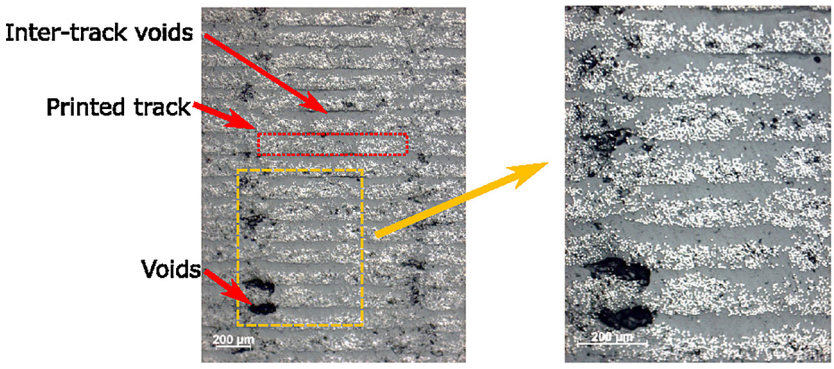

Fig. 13. Cross section of printed MarkForged part showing structure from 3D printing tracks and distribution of voids.

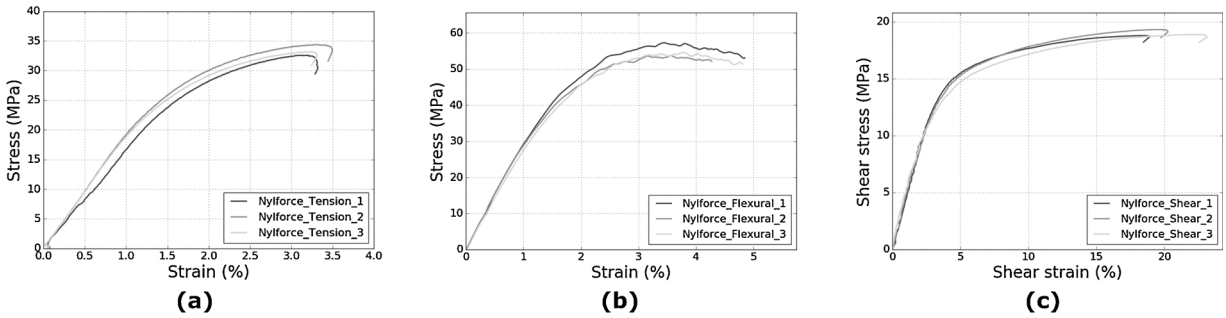

Fig. 14. (a) Tensile, (b) flexural and (c) shear test results of carbon microfibre reinforced Nylon.

coherent understanding of how different printing parameters affect final part quality.

The ideal properties for a 3D printing filament are summed up in Table 3, categorized into processing and performance properties. The flow properties of the polymer are important for the polymer sintering process, which ideally consists of a low melt viscosity and high surface energy. The thermal properties of a 3D printing filament dictate the thermal energy history of the printed tracks, where it is important that the extruded material and the surrounding material reach a high enough temperature and maintain that temperature for long enough to enable bonding between adjacent tracks. A higher heat capacity means the material needs more heat input to increase its temperature but can also store more heat once it leaves the liquefier, while a high conductivity is required to transfer the heat to the surrounding material. After sintering, the material cools down which may induce residual stresses, so ideally the material has a low melt/glass transition temperature, which is a conflicting requirement with a high operating temperature. The desired mechanical properties of the polymer are a high stiffness and strength, and potentially a good interfacial strength when reinforcing fibres are used.

Studies indicated that the addition of fibres to the filament may improve the heat transfer between printed tracks, leading to a better sintering process and reducing void content. However, fibres also increase the viscosity of the melt which has a negative effect on the sintering process as some studies showed a higher void content with fibres. A larger, more extensive study is proposed wherein the effect of different fillers, printing temperatures and printing strategies are investigated in order to reduce the void content and obtain higher quality parts.

Another important aspect for the printing of composite materials is the use of short versus continuous fibres. Currently, a limited number of commercial products are available for both, but rigorous, comparative material testing with detailed consideration of defects (through optical microscopy) has until now not been available in the public domain. The test results of the MarkOne continuous fibre printed parts presented here indicate good mechanical properties which are an order of magnitude higher than typical FFF printed materials, although still

Table 2
Comparison printing methods with normalised mechanical properties to fibre volume content of 15%.

	Short fibre printing method		Continuous fibre printing method	
Brand name	Nylforce		MarkForged	
Fibre volume content	6%		27%	
Porosity	1.1%		9%	
	Measured	*Normalised*	*Measured*	*Normalised*
Tensile modulus [GPa]	1.85	4.6	62.5	46.9
Tensile strength [MPa]	33.5	83.8	968	726.0
Flexural modulus [GPa]	3	7.5	41.6	31.2
Flexural strength [MPa]	55.3	138.3	485	363.8
Shear modulus [GPa]	0.31	0.8	2.26	1.7
Shear strength [MPa]	19	47.5	31.16	23.4

significantly lower than unidirectional composites made with traditional manufacturing methods (strength/stiffness of 1500 MPa/135 GPa). Placement of continuous fibre filament is limited by a number of geometric and processing constraints, such as a minimal deposition length and minimal corner radii. Short fibre printing allows for considerably more freedom in where and how the reinforcement is placed, resulting in easier processing of the material and lower void content. The mechanical properties are relatively low as the matrix or fibre-matrix interface fails before the fibres.

The results agree with the known trade-off between processing and performance as shown in Fig. 16. To further optimize fibre reinforced 3D printing materials, highly aligned short fibres with fibres above the critical fibre length may provide a good trade-off between processing and performance. For carbon fibre in a Nylon matrix, the critical fibre length is roughly 0.5 mm [46]. Investigations have shown that aligned short fibre / epoxy composites (V_f = 55%) can obtain a strength and stiffness of 1500 MPa and 115 GPa with the HiPerDiF method [48,49]. Increasing the fibre length therefore may be a way forward to an 3D printing filament with the advantages of rapid prototyping and compete with continuous fibre mechanical performance.

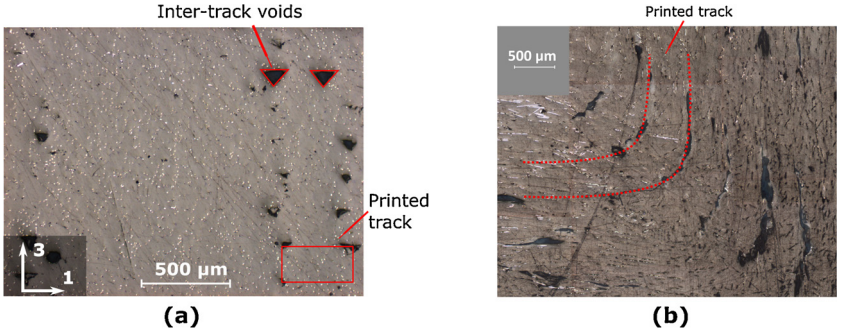

Fig. 15. Microstructure of 3D printed short fibre Nylon showing (a) cross section and (b) top view of corner.

Table 3
Overview of desired properties for a fibre reinforced 3D printing filament.

Processing properties	Melt viscosity	Low melt viscosity for easy flow of the polymer
	Surface energy	High surface energy to improve polymer sintering process
	Melt temperature	Low melt temperature for lower residual stresses
	Heat capacity	High heat capacity to better retain temperature after printing
	Heat conductivity	High heat conductivity to transfer heat through the printed part
Mechanical performance properties	Stiffness/strength	High stiffness and strength for overall mechanical performance
	Interfacial strength	Good interfacial strength with reinforcing fibres
	Operating temperature	High operating temperature before becoming glassy

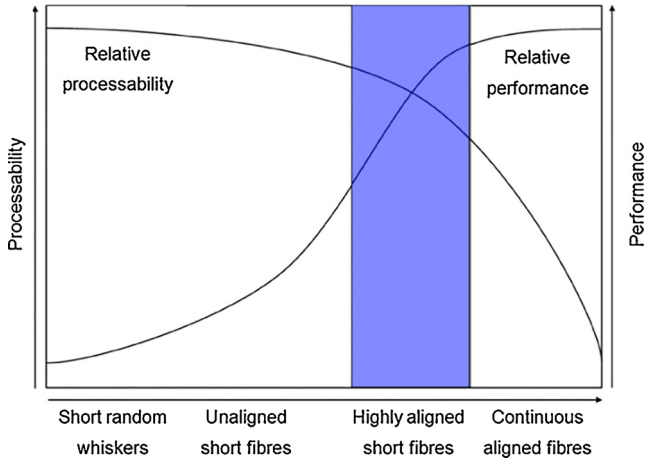

Fig. 16. Impact of fibre architecture on processability and performance [47].

6. Conclusions

In this work the state of the art of 3D printed composite parts has been presented, and the performance of two of the most advanced solutions currently available have been benchmarked with mechanical testing and optical microscopy. Printing of short fibre (~0.1 mm) reinforced Nylon filament was performed using a standard open-source FFF printer and a MarkOne 3D printer was used to print continuous carbon fibre / Nylon composite specimens. The tensile strength and stiffness of the continuous fibre printed parts were 986 MPa and 64 GPa respectively, which is more than an order of magnitude higher than the short fibre reinforced Nylon printed parts (33 MPa and 1.9 GPa). A disadvantage of the continuous fibre printer, however, is limited control over the placement of the fibre and the creation of voids when printing more complex shapes. To overcome these disadvantages, a thermoplastic filament reinforced with short fibres above the critical fibre length is proposed. This would yield mechanical properties similar to continuous fibre prints while maintaining the better processing qualities of short fibre reinforced filament. This may enable new applications for high performance 3D printed parts suitable for medical, aerospace, sport and rapid prototyping applications.

Acknowledgements

This work was supported by the Engineering and Physical Sciences Research Council through the ACCIS Doctoral Training Centre [grant number EP/G036772/1]. Data access statement All underlying data supporting the conclusions are provided in full within this paper.

References

[1] A. Mouritz, Introduction to Aerospace Materials, First ed., Woodhead Publishing Ltd, Cambridge, England, 2012.
[2] Markforged, High Strength 3D Printing With Continuous Fibres, [Online]. Available: (2016) [Accessed: 01-Nov-2016] https://markforged.com/.
[3] Q. Sun, C. Bellehumeur, P. Gu, Effect of processing conditions on the bonding quality of FDM polymer filament," solid Free, Fabr. Proc. 14 (403) (2002) 400–407.
[4] B.N. Turner, S.A. Gold, A review of melt extrusion additive manufacturing processes: II. Materials, dimensional accuracy, and surface roughness, Rapid Prototyp. J. 21 (3) (2015) 250–261.
[5] J.T. Belter, A.M. Dollar, Strengthening of 3D printed fused deposition manufactured parts using the fill compositing technique, PLoS One 10 (4) (2015) 1–19.
[6] J.F. Rodriguez, J.P. Thomas, J.E. Renaud, J.F. Rodriguez, J.P. Thomas, J.E. Renaud, J.F. Rodriguez, J.P. Thomas, J.E. Renaud, Characterization of the Mesostructure of Fused-Deposition Acrylonitrile-Butadiene-Styrene Materials, (2011).
[7] B.N. Turner, R. Strong, S.A. Gold, A review of melt extrusion additive manufacturing processes: I. Process design and modeling, Rapid Prototyp. J. 20 (3) (2014) 192–204.
[8] S. Ahn, M. Montero, D. Odell, S. Roundy, P.K. Wright, Anisotropic material properties of fused deposition modeling ABS, Rapid Prototyp. J. 8 (4) (2002) 248–257.
[9] L. Li, Q. Sun, C. Bellehumeur, P. Gu, Investigation of bond formation in FDM process," solid free, Fabr. Proc. (403) (2002) 400–407.
[10] W. Wu, P. Geng, G. Li, D. Zhao, H. Zhang, J. Zhao, Influence of layer thickness and raster angle on the mechanical properties of 3D-printed PEEK and a comparative mechanical study between PEEK and ABS, Materials (Basel) 8 (9) (2015) 5834–5846.
[11] B. Huang, S. Singamneni, Raster angle mechanics in fused deposition modelling, J. Compos. Mater. 0 (January) (2014) 1–21.
[12] J. Rodriguez, maximizing the strength of fused-deposition ABS plastic parts, 10th Solid Free, (1999), pp. 335–342.
[13] L. Li, Q. Sun, C. Bellehumeur, P. Gu, Composite modeling and analysis for fabrication of FDM prototypes with locally controlled properties, J. Manuf. Process. 4 (2) (2002) 129–141.
[14] M.A. Yardimci, S.I. Guceri, M. Agarwala, S.C. Danforth, Part quality prediction tools for fused deposition processing, Proceedings of the Solid Freeform Fabrication Symposium, (1996), pp. 539–548.
[15] M.A. Yardimci, T. Hattori, S.I. Guceri, S.C. Danforth, Thermal analysis of fused deposition Sept. 1997, Solid Free. Fabr. Proceedings, (1997), pp. 689–698.
[16] C. Bellehumeur, L. Li, Q. Sun, P. Gu, modeling of bond formation between polymer filaments in the fused deposition modeling process, J. Manuf. Process. 6 (2) (2004) 170–178.
[17] O. Pokluda, C.T. Bellehumeur, J. Machopoulos, Modification of Frenkel's model for sintering, AIChE J. 43 (12) (1997) 3253–3256.
[18] A. Bellini, Fused Deposition of Ceramics : A Comprehensive Experimental, Analytical and Computational Study of Material Behavior, Fabrication Process and Equipment Design, Drexel University, 2002.
[19] A. Lanzotti, M. Grasso, G. Staiano, M. Martorelli, The impact of process parameters on mechanical properties of parts fabricated in PLA with an open-source 3-D printer, Rapid Prototyp. J. 5 (2015) 604–617.
[20] K.G.J. Christiyan, U. Chandrasekhar, K. Venkateswarlu, A study on the influence of process parameters on the mechanical properties of 3D printed ABS composite, IOP Conf. Ser.: Mater. Sci. Eng. 114 (2016) 1–8.
[21] S. Hwang, E.I. Reyes, K. Moon, R.C. Rumpf, N.A.M.S.O.O. Kim, Thermo-mechanical characterization of metal / polymer composite filaments and printing parameter study for fused deposition modeling in the 3D printing process, J. Electron. Mater. 44 (3) (2015) 11664.
[22] U. Kalsoom, P.N. Nesterenko, B. Paull, Recent developments in 3D printable composite materials, RSC Adv. 6 (65) (2016) 60355–60371.
[23] X. Wang, M. Jiang, Z. Zhou, J. Gou, D. Hui, 3D printing of polymer matrix composites: a review and prospective, Compos. Part B Eng. 110 (2017) 442–458.
[24] F. Ning, W. Cong, J. Qiu, J. Wei, S. Wang, Additive manufacturing of carbon fiber reinforced thermoplastic composites using fused deposition modeling, Compos. Part B Eng. 80 (2015) 369–378.
[25] H.L. Tekinalp, V. Kunc, G.M. Velez-Garcia, C.E. Duty, L.J. Love, A.K. Naskar, C.A. Blue, S. Ozcan, Highly oriented carbon fiber-polymer composites via additive manufacturing, Compos. Sci. Technol. 105 (2014) 144–150.
[26] R. Matsuzaki, M. Ueda, M. Namiki, T.-K. Jeong, H. Asahara, K. Horiguchi, T. Nakamura, A. Todoroki, Y. Hirano, Three-dimensional printing of continuous-fiber composites by in-nozzle impregnation, Sci. Rep. 6 (February) (2016) 23058.
[27] M.L. Shofner, K. Lozano, F.J. Rodríguez-Macías, E.V. Barrera, Nanofiber-reinforced polymers prepared by fused deposition modeling, J. Appl. Polym. Sci. 89 (11) (2003) 3081–3090.
[28] C. Mahajan, D. Cormier, 3D printing of carbon fiber composites with preferentially aligned fibers, Proc. 2015 Ind. Syst. Eng. Reserach Conf. (2015).
[29] J. Peng, T.L. Lin, P. Calvert, Orientation effects in freeformed short-fiber composites, Compos. Part A Appl. Sci. Manuf. 30 (1999) 133–138.
[31] J.P. Lewicki, J.N. Rodriguez, C. Zhu, M.A. Worsley, A.S. Wu, Y. Kanarska, J.D. Horn, E.B. Duoss, J.M. Ortega, W. Elmer, R. Hensleigh, R.A. Fellini, M.J. King, 3D-Printing of meso-structurally ordered carbon fiber/polymer composites with

unprecedented orthotropic physical properties, Sci. Rep. 7 (December) (2017) 43401 2016.
[32] M.L. Longana, N. Ong, H. Yu, K.D. Potter, Multiple closed loop recycling of carbon fibre composites with the HiPerDiF (High performance discontinuous fibre) method, Compos. Struct. 153 (2016) 271–277.
[33] S.Y. Fu, B. Lauke, Effects of fiber length and fiber orientation distributions on the tensile strength of short-fiber-reinforced polymers, Compos. Sci. Technol. 56 (10) (1996) 1179–1190.
[34] W. Zhang, A.S. Wu, J. Sun, Z. Quan, B. Gu, B. Sun, C. Cotton, D. Heider, T.W. Chou, Characterization of residual stress and deformation in additively manufactured ABS polymer and composite specimens, Compos. Sci. Technol. 150 (2017) 102–110.
[35] F. Ning, W. Cong, J. Qiu, J. Wei, S. Wang, Additive manufacturing of carbon fiber reinforced thermoplastic composites using fused deposition modeling, Compos. Part B Eng. 80 (2015) 369–378.
[36] C. Yang, X. Tian, T. Liu, Y. Cao, D. Li, 3D printing for continuous fiber reinforced thermoplastic composites: mechanism and performance, Rapid Prototyp. J. 23 (1) (2017) 209–215.
[37] D. Valentin, F. Paray, B. Guetta, The hygrothermal behaviour of glass fibre reinforced Pa66 composites: a study of the effect of water absorption on their mechanical properties, J. Mater. Sci. 22 (1) (1987) 46–56.
[38] ASTM International, D3039/D3039M: Standard Test Method for Tensile Properties of Polymer Matrix Composite Materials, (2014), pp. 1–13.
[39] ASTM International, D7264/D7264M-07: Standard Test Method for Flexural Properties of Polymer Matrix Composite Materials 1, (2010), pp. 1–11.
[40] C.T. Sun, I. Chung, An oblique end-tab design for testing off-axis composite specimens, Composites 24 (8) (1993) 619–623.
[41] Fiber Force Italy, Technical Data Sheet – Nylforce Carbon Fibe, Treviso, Italy (2017), p. 1.
[42] ASTM International, D638: Standard Test Method for Tensile Properties of Plastics, (2013), pp. 1–16.
[43] M.R. Wisnom, The relationship between tensile and flexural strength of unidirectional composites, J. Compos. Mater. 26 (8) (1992) 1173–1180.
[44] A. Lanzotti, M. Grasso, G. Staiano, M. Martorelli, The impact of process parameters on mechanical properties of parts fabricated in PLA with an open-source 3-D printer, Rapid Prototyp. J. 21 (5) (2015) 604–617.
[45] D.H.J. a Lukaszewicz, C. Ward, K.D. Potter, The engineering aspects of automated prepreg layup: history, present and future, Compos. Part B Eng. 43 (3) (2012) 997–1009.
[46] P.D. Shipton, The Compounding Of Short Fibre Reinforced Thermoplastic Composites, Brunel University, 1988.
[47] M. Such, C. Ward, K. Potter, Aligned discontinuous fibre composites: a short history, J. Multifunct. Compos. 2 (3) (2014) 155–168.
[48] H. Yu, K.D. Potter, M.R. Wisnom, A novel manufacturing method for aligned discontinuous fibre composites (High performance-discontinuous fibre method, Compos. Part A Appl. Sci. Manuf. 65 (2014) 175–185.
[49] M.L. Longana, H. Yu, K.D. Potter, Aligned short fibre hybrid composites with virgin and recycled carbon fibres, Proceedings of the 20th International Conference on Composite Materials (ICCM20). International Conference on Composite Materials, ICCM, (2015).